Gamma Camera - advantages and limits identifying sources over a broad energy range

M. Risse, S. Chmel, H. Friedrich, T. Köble, O. Schumann, T. Teuteberg
Fraunhofer INT, Appelsgarten 2, 53879 Euskirchen, Germany

1 ABSTRACT

Radioactive or nuclear material could fall into the wrong hands and pose a serious threat to society. If it is suspected that this type of radioactive or nuclear material is present in an area, it is necessary to locate it and identify any material found. Especially in the case of nuclear material involved there is an urgent need to identify and classify the material. To do this simultaneously and within the shortest possible time, gamma cameras are used. It is of great interest to investigate the limits and characteristics of this kind of non-destructive technology. This paper presents the results of tests carried out with NUVIA's NuVISION, a mobile spectrometric gamma imaging system equipped with a cadmium zinc telluride (CZT) detector. It comprises a high-resolution capability using a coded mask and a 360° field of view (FOV) using Compton imaging. The fast signal processing enables real-time display of the measurement results. The orientation of the measurement system can be controlled remotely by rotation of the detection head in three axes.

The sensitivity of CZT detectors is relatively low at higher energies, therefore the detection of ^{60}Co with energies of 1173 keV and 1332 keV is of particular interest. The difference in performance for radioactive materials covering the energy range from ^{241}Am to ^{60}Co is investigated. Moreover, the spatial distribution is analyzed in order to investigate the geometric sensitivity from the Compton imaging. The influence of different shielding material on the performance of the gamma camera is also studied. In addition, the dependence of the measurement time on the quality of the measurement results is investigated.

Key words: Gamma camera, Compton imaging, coded Mask, Energy dependence of measurement result, shielding material, identification, localization.

2 INTRODUCTION

The accurate localization of radioactive and nuclear materials is an important task for nuclear safety and security. In addition to the possibility of scanning an area with handheld devices, imaging methods can also be used. Two different approaches here are Compton and Coded Mask imaging. A Compton camera [1] uses the Compton scattering effect to determine the direction of incoming radiation. Typically, it consists of two main detectors, the scatter detector and the absorber detector. In the first layer the incident gamma ray has a Compton scattering event and might not be absorbed within. The scattered gamma from the first layer is completely absorbed in the second detector. The location of the interaction and energy of interacting photons in the layers are detected and a back-projection of probability cone of source locations is done. For a full 360° field of view a symmetrical structure will have to be used. The coded-aperture approach for radiation detection has its roots in development of scatter-hole cameras for X- and gamma rays and has widely been used in medicine [2]. It consists of two main components, a coded aperture (mask) and a detector plane behind the mask. The mask is a plate with a specific pattern of transparent and opaque regions. They are arranged according to a mathematic code which ensures

that the pattern is non-redundant and can be used to reconstruct an image accurately. Both systems are combined in the Gamma camera NuVISION [4]. It provides a 360° FOV via the Compton imaging with a 15° spatial resolution as well as a good 3.5° resolution due to the coded mask imaging in a 45° FOV. In here a tungsten mask is used. Due to the use of a CZT detector an identification is possible and the spectrometric capacity of the camera shall cover an energy range from 20 keV to 1400 keV.
In the present paper the NuVISION device is used to develop principle performances of Compton and coded mask imaging as well as the identification. In order to test the performance over the whole energy range different radioactive sources have been used. In a first step the shielding effects of the own device are studied. This includes shielding by the coded mask made of tungsten, the holder and, in the case of measurements from the rear side, the electronics. Scans with all sources are performed.

3 SETUP AND PERFORMANCE

The NuVISION is mounted on a motorized holder which can be remote-controlled and enables a scanning. A switch between the two imaging methods "Coded Mask Imaging" and "Compton Imaging" is possible at any time, even during an ongoing measurement. According to the data sheet the localization time with a natural background depends on the dose rate caused by the hotspots on the detector: a few seconds for dose rates in the µSv/h range and a few minutes in the range from 50 to a few hundred nSv/h. The spatial measurement result is overlaid with an optical image. Parallax correction is not necessary, as gamma and visual image have the same alignment, but there is a small offset which is particularly noticeable at short distances.

The given distances of the measurements are related to the detector position which is next to the holder position, see Figure 1. The detector is positioned with a motorized holder which enables an automated scan.

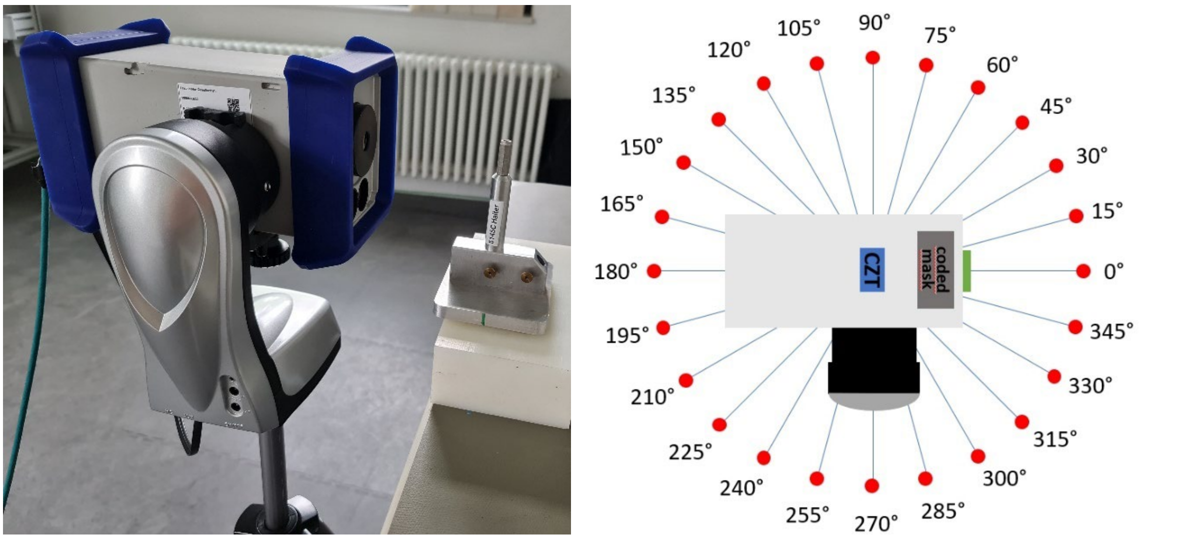

Figure 1: <u>Left:</u> NuVision camera on the motorized holder in front of a source at 0°. <u>Right:</u> Top view sketch of the detector. Given distances are towards the point of the detector. The detector is located at the intersection of the 0°/180° and 90°/270° lines next to the holder. The dots mark the position of the sources, the corresponding angle for the measurement situation is given as well. Green: optical camera; Black: motorized holder; Blue: CZT detector; Grey: tungsten mask.

4 RADIOACTIVE SOURCES

Five nuclides are investigated in the framework of the paper covering the whole energy range: ^{241}Am, ^{133}Ba, ^{152}Eu, ^{137}Cs and ^{60}Co. Table 1 lists the kind of the source, the internal label, the dose rate measured in 30 cm distance, the activity and the main energy lines.

nuclide	label	dose rate [µSv/h]	activity [kBq]	main energy lines [keV]
^{241}Am	AO8787	0.16	1800	59.54
^{133}Ba	AF8795	0.68	560	81.0; 276.4; 302.9; 356.0; 383.8
^{152}Eu	AF8796	1.25	600	121.8; 244.7; 344.3; 778.9; 964.0
^{137}Cs	BE1403	3.02	3600	661.6
^{137}Cs	NH233	2.18	2380	661.6
^{60}Co	5145C	0.42	145	1173.2; 1332.5

Table 1: Summary of the radioactive sources. The first column states the kind of source followed with the internal label, the measured dose rate in 30 cm and activity at the date of the measurement. The BE1403 source was used throughout for ^{137}Cs measurements, the NH233 source was only applied when two ^{137}Cs sources were used for the same measurement.

5 MEASUREMENTS AND TEST RESULTS

5.1 Counts in dependence on the position

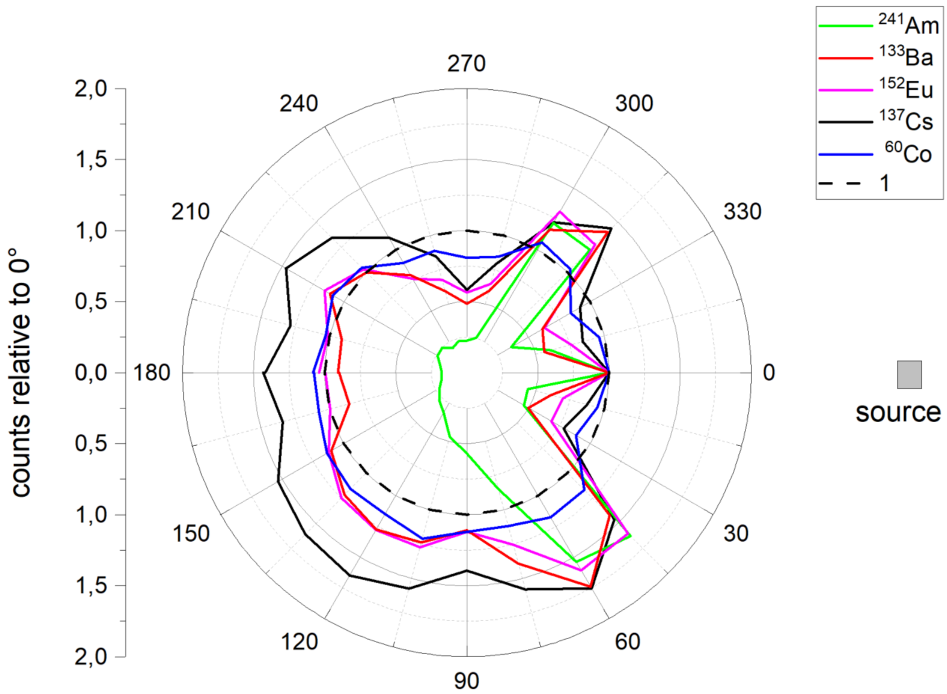

Figure 2: Polar diagram of all scans counts relative to the measurement in the direction of the source. Measurement duration 60 s, distance 30 cm, measuring increment 15°. The given angles are defined like in Figure 1. The dashed line represents an isotropic distribution.

The Polar diagram in Figure 2 shows the results of all scans for the different nuclides. The orientation of the detector towards the sources are like given in Figure 1. In order to compare the measurement results the counts are normalized towards the measurement at 0° in the direction of the source. If the counts measured in all orientations were the same a circle with radius 1 would result. This is marked with the black dashed line. The measurement with the nuclide of the highest gamma energies ^{60}Co is the closest to the isotropic case. For ^{60}Co the shielding effect of the coded mask, the motorized holder and the other detector material is the smallest. For the nuclide with the lowest gamma energy ^{241}Am the shielding effect is highest and indicates the shielding effect best. At 180° from the back, the radiation is shielded through the detector materials like cable, electronics etc. Around 15° and 30° the shielding effect of the coded mask made of tungsten is highest. Between 45° and 60° the radiation hits the CZT detector with the least shielding, the coded mask is no longer transmitted. The measured value is even higher than the value at 0° because the coded mask's shielding effect is removed. The measurement is not symmetric as during measurements between 180° and 0° the motorized holder is in between.

5.2 Images

The specific pattern in the Compton image bases on the source's position relative to the detector. Figure 3 shows the images for a 300 s measurement in 30 cm distance obtained with the ^{137}Cs source. In the left part the whole Compton image is shown, the two red circles with the dashed lines indicate 90° sphere (inner) which is perpendicular to the direction of view and 180° sphere (outer) which is backwards. The direction (bottom, top, left and right) can directly be taken from the position in the image. For single sources the pattern is:

- For sources at angles between 0° and 90° with respect to the direction of view (corresponds to positions in the range 270° to 90° in Figure 1) a single spot indicates the position within the first circle.
- For sources at angles between 90° and 180° with respect to the direction of view (corresponds to positions in the range 90° to 270° in Figure 1), two distinct spots will be observed one inside the inner circle which is a "phantom spot" and one between the two circles.
- When the source is directly behind the detector, opposite to the direction of the optical camera, it will appear as a circle in the opposite direction.

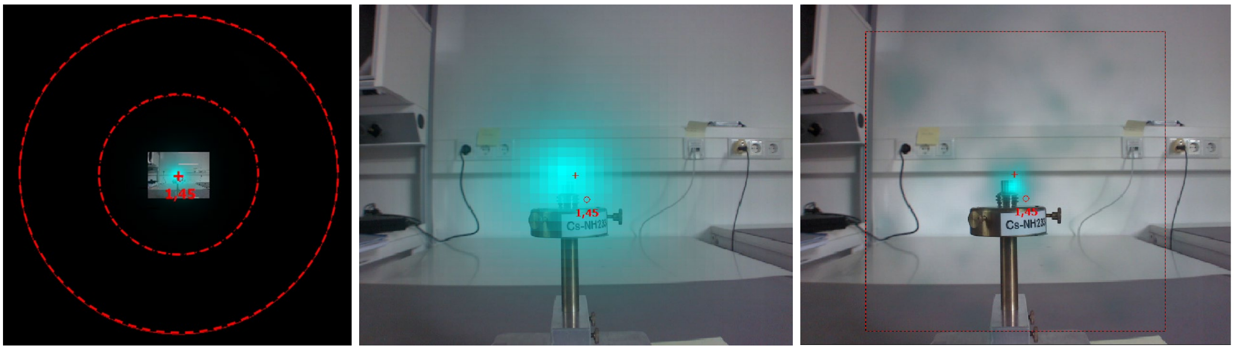

Figure 3: ^{137}Cs source for 300 s in a distance of 30 cm. Left: Compton image 360°, inner red circle: 90° (perpendicular), outer red circle: 180° (backwards). Middle: Compton image zoomed. Right: Coded Mask image. The red square marks the 45° field of view.

The result of the coded mask imaging is given, too. The red square marks the 45° FOV. The lower spatial resolution in the Compton imaging is obvious due to the larger size of the spot. A color code is used to indicate the identification result: ^{137}Cs: cyan, ^{241}Am: magenta, ^{133}Ba: green, ^{152}Eu: dark blue, ^{60}Co: yellow. In both images a cross indicates the center of the image and an open circle the position of the distance measurement. The evaluated distance is given. In this case the distance is not towards the source but next to the source towards the wall in the back.

Compton images from a horizontal scan are given in Figure 4. They illustrate the pattern described above and clearly indicate the position of the source in every image, also showing the aforementioned “phantom spot” for sources at an angle >90° with respect to the line of view. A solution could be to perform a second measurement with the detector turned horizontal for 180°.

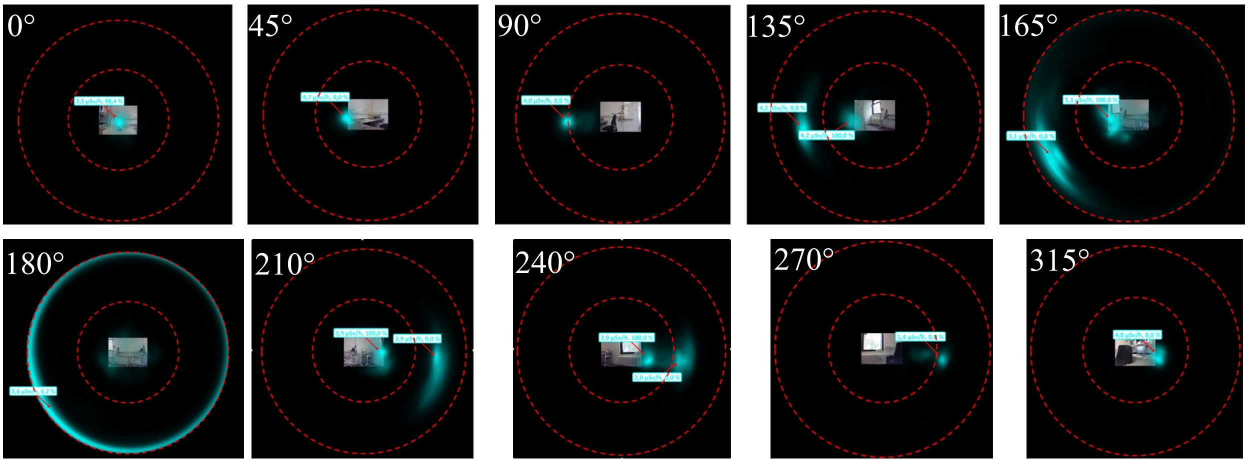

Figure 4: Compton images obtained with the ^{137}Cs source, measurement duration 60 s. The geometry is as in Figure 1 and indicated in the images. In the center of the 0° picture the source is situated. Between 90° and 270° the indication is split in two parts, one “phantom spot” inside the inner circle and the real location between the two lines.

The results obtained for ^{137}Cs are good, whereas results obtained with other nuclides do not have the same quality, as seen for ^{241}Am in Figure 5. The sources differ in source strength and the gamma energy like given in Table 1.

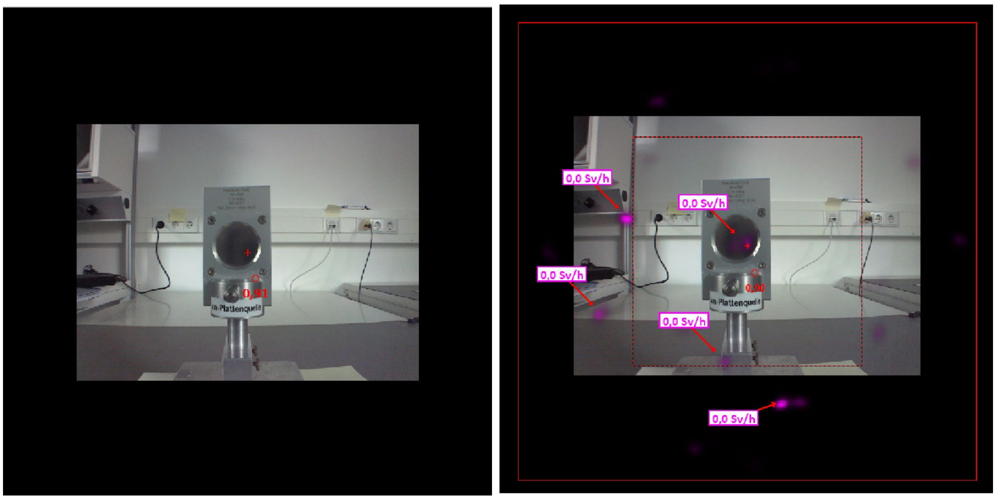

Figure 5: ^{241}Am source for 310 s in a distance of 30 cm. Left: Compton image. Right: Coded Mask image. The position of the source is not detected.

In addition to the measurements with individual sources, measurements with two sources were also carried out. This included two sources with the same nuclide (both ^{137}Cs, as these are the strongest sources) and two different sources (^{137}Cs and ^{152}Eu, with ^{152}Eu chosen because it, along with the ^{137}Cs source, yielded the best results in terms of identification as shown in Table 2).

Figure 6 and Figure 7 show the Compton and Coded Mask images at 0°. In Figure 6, both sources are placed at a distance of 100 cm and are 60 cm apart. Therefore, they have different dose rates. In the Compton image, a single spot is visible that does not resolve the two sources but shows only one spot. In the Coded Mask image, only one source is visible as a single spot, with the stronger BE1403 source correctly marked, while the slightly weaker source is not marked. Subsequently, the distances were adjusted so that both sources yield the same dose rate at the detector position, the result is given in Figure 7. In the Coded Mask image, both positions are now marked with a spot, but there are still additional blemishes in the image. In the Compton image, two spots could be perceived, but it is not entirely clear.

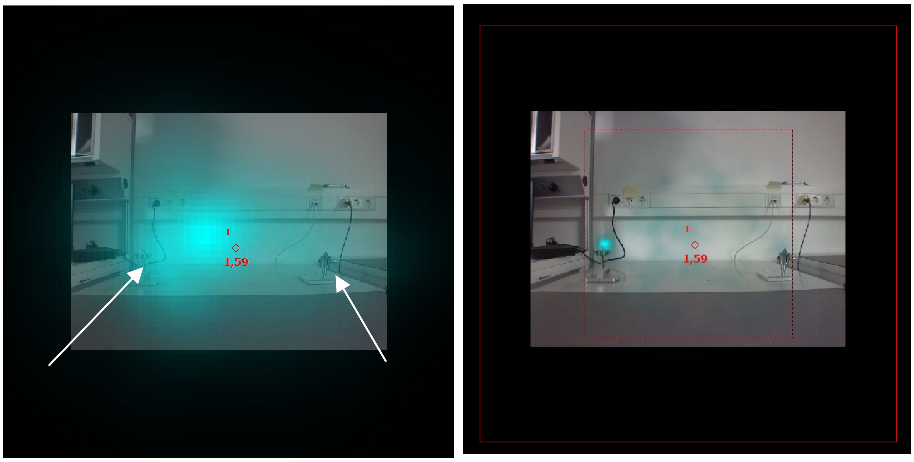

Figure 6: Two ^{137}Cs sources in 100 cm each, sources marked with the white arrows are 60 cm apart. The left one is BE1403, the right one NH233. Measurement time 2400 s. Left: Compton imaging. Right: Mask imaging.

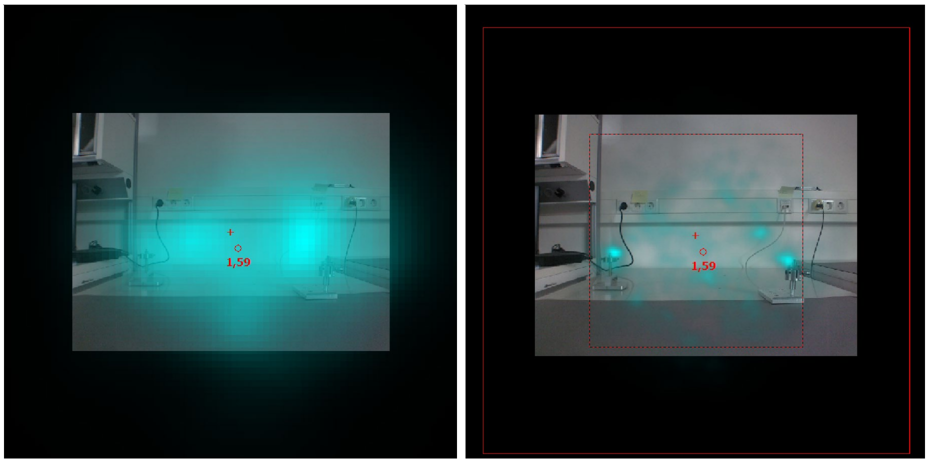

Figure 7: Two ^{137}Cs sources, BE1403 in 102 cm and NH233 in 80 cm distance, sources are 57 cm apart from each other. Measurement time 600 s. Left: Compton imaging. Right: Mask imaging. Source distances are adjusted to yield the same dose rate at the detector position.

Figure 8 shows the results for the different sources, ^{137}Cs and ^{152}Eu. The distances between the sources are chosen so that the dose rates at the detector position are equal. The two sources are well separated by the different colors: cyan for ^{137}Cs and blue for ^{152}Eu. In the Compton image, however, the centers of the spots are not at the positions of the sources, but in the right direction and well separated due to the colors. In the Coded Mask image, the sources are very well localized.

The spot for the ^{137}Cs source aligns very well with the optical image, while the position of the ^{152}Eu source is slightly offset (optical image and γ-ray signal).

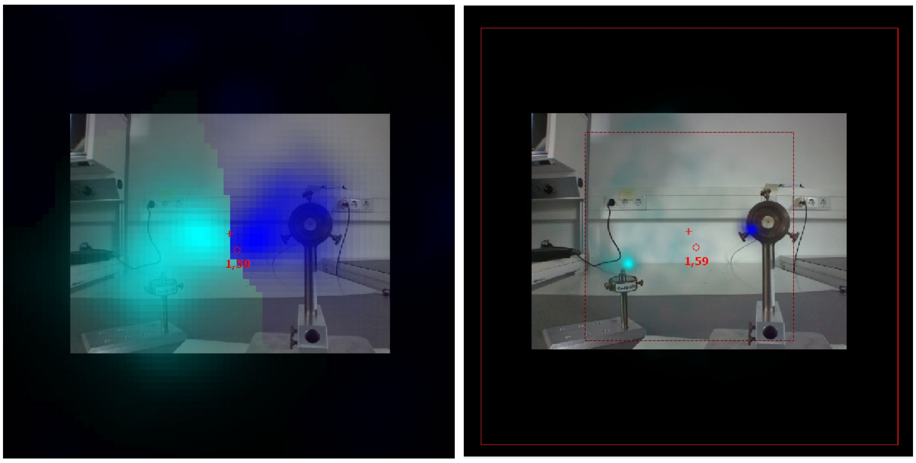

Figure 8: ^{137}Cs in 48 cm, ^{152}Eu in 30 cm distance, sources are 25 cm apart from each other, measurement time 300 s. ^{137}Cs is located a bit lower. The position is a bit offset (optical image and γ signal), cyan: ^{137}Cs, blue: ^{152}Eu. Left: Compton imaging. Right: Mask imaging. Source distances are adjusted to yield the same dose rate at the detector position.

5.3 Identification

The identification of the measured sources is done by evaluation of the gamma spectra which are shown in Figure 10. The CZT detector is less efficient at high energies which can well be seen from the ^{60}Co spectrum. Peaks are hardly distinguishable from the background and significantly lower than the low-energy background. Spectra of ^{241}Am und ^{133}Ba show a much better signal-to-noise ratio of their low-energy peaks. The ^{137}Cs medium-energy peak is still clearly distinguishable, but it is not higher than the low-energy background. Nevertheless, the peak probably is distinct enough to allow for fitting to it and, thus, identification of the nuclide.

The identification results have been considered for all scans. Exemplarily, the results for ^{241}Am are also included in the polar diagram of the counts, see Figure 10. The results are categorized as follows: ■ ^{241}Am: ^{241}Am is identified, □ ^{241}Am +: ^{241}Am and something else are identified, ▲ others: no ^{241}Am is identified but something else is. "Something else" can be another nuclide or a specific gamma line. If no identification occurs, nothing is indicated. It is evident that the identification result correlates with the counts or the change in the spectrum caused by shielding. In the backward direction, no ^{241}Am is identified between 135° and 195°.

Identification results for the scans with all nuclides are shown in Table 2. The results are also given in the three previously mentioned categories. Results that provide the correct identification are marked in green. Results in blue indicate that the nuclide is identified, but something else is also identified. In red, in the row labeled "o," others are indicated. Here, the nuclide is not identified, but a different nuclide or other energy lines are identified. It is evident that the result for ^{60}Co is the worst; ^{60}Co is never identified. This is due to the poor efficiency in the higher energy range. ^{137}Cs is identified in every measurement, and in 20 out of 25 cases, ^{241}Am is also identified. The spectrum shows in this range also a small peak at about 60 keV. At around 57-70 keV, the K-lines of the characteristic X-ray radiation of tungsten, the material of the mask, are located. This could be due to ionization in tungsten. ^{152}Eu is identified in 24 out of 25 cases, with 19 of those cases being the sole identification result. Here too, the results are better in the forward direction than in the backward direction. However, unlike the results for ^{137}Cs, only at 285° ^{241}Am is also identified. In the case of ^{133}Ba, the identification result is also better in the forward direction. In the range from 150° to 270°, ^{133}Ba is only identified at 225°.

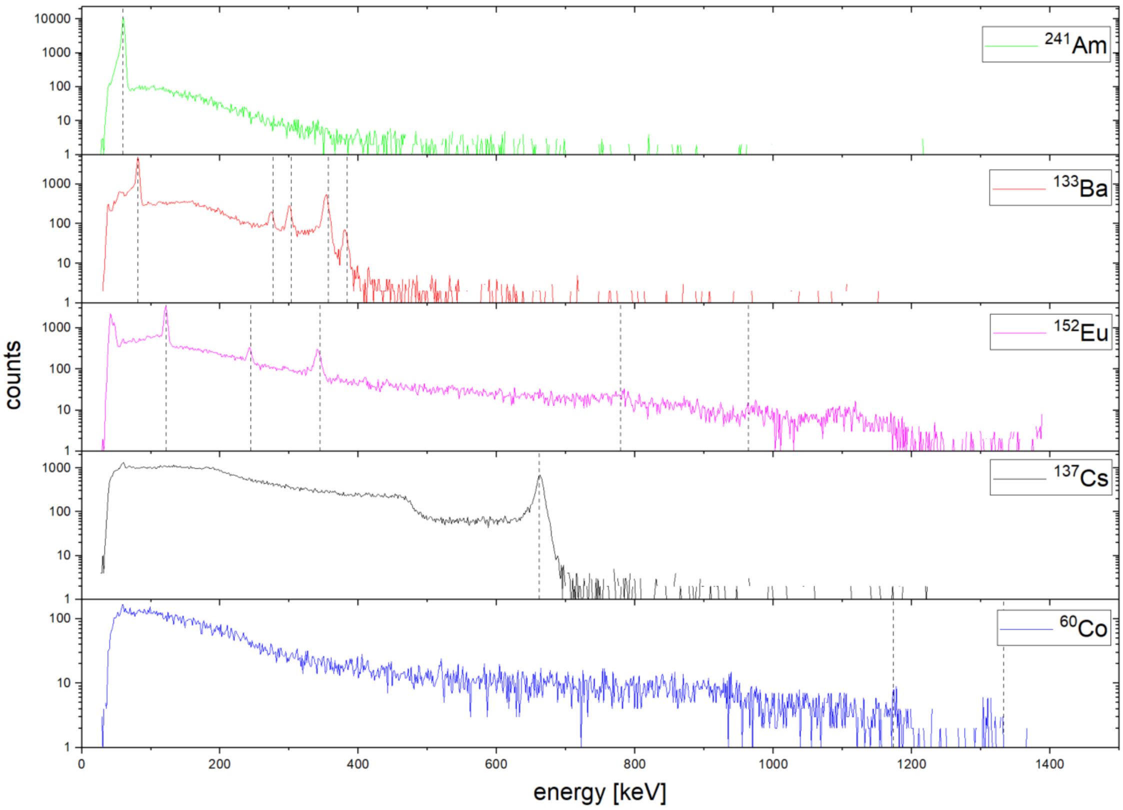

Figure 9: Gamma Spectra for all 5 different sources like given in Table 1. The main gamma energies are indicated by the dashed lines. In all cases the sources are measured for 300 s in a distance of 30 cm.

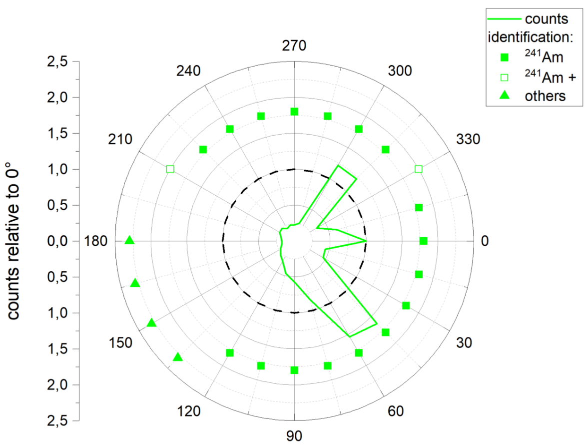

Figure 10: ^{241}Am results, counts relative to 0° position like displayed in Figure 2 and in addition the identification result. ■ ^{241}Am: ^{241}Am is identified, □ ^{241}Am +: ^{241}Am and something else are identified, ▲ others: no ^{241}Am is identified but something else. Something else can be another nuclide or a specific gamma line.

Position [°]		180	195	210	225	240	255	270	285	300	315	330	345	0	15	30	45	60	75	90	105	120	135	150	165	180
^{241}Am	Am				x	x	x	x	x	x	x		x	x	x	x	x	x	x	x	x	x				
	Am+			x								x														
	o	x																					x	x	x	x
^{133}Ba	Ba											x	x		x					x	x	x				
	Ba+				x				x	x	x			x		x	x	x	x				x			
	o	x	x	x		x	x	x																x	x	x
^{152}Eu	Eu			x	x		x	x		x	x	x	x		x	x	x	x	x		x		x		x	
	Eu+	x	x						x					x						x		x		x		x
	o					x																				
^{137}Cs	Cs			x				x				x							x			x				
	Cs+	x	x		x	x	x		x	x	x		x	x	x	x	x	x		x	x		x	x	x	x
	o																									
^{60}Co	Co																									
	Co+																									
	o	x		x				x			x	x			x			x			x	x			x	

Table 2: Summary of identification results for all measured nuclides. The position in the first line is like given in Figure 1. The following lines give the identification results. Am, Ba, Eu, Cs and Co indicate that the nuclide is correctly identified alone. The additional + indicates that the nuclide is correctly identified along with other elements (o = others). o means that only other elements are identified. Others can be a different nuclide or a specific gamma energy. If nothing is identified, no entry is recorded.

5.4 Count rate

In the polar diagram in Figure 2 the counts relative to the counts measured in the source direction of 0° are plotted. In contrast, Figure 11 shows the measured count rates of all sources versus the angle. During the measurements with ^{60}Co it was never identified and no source was located. However, the presence of a source can be realized when looking at the count rate. It is nearly constant during the scan, but the measurement value is higher than during background measurement and still indicates the presence of a source.

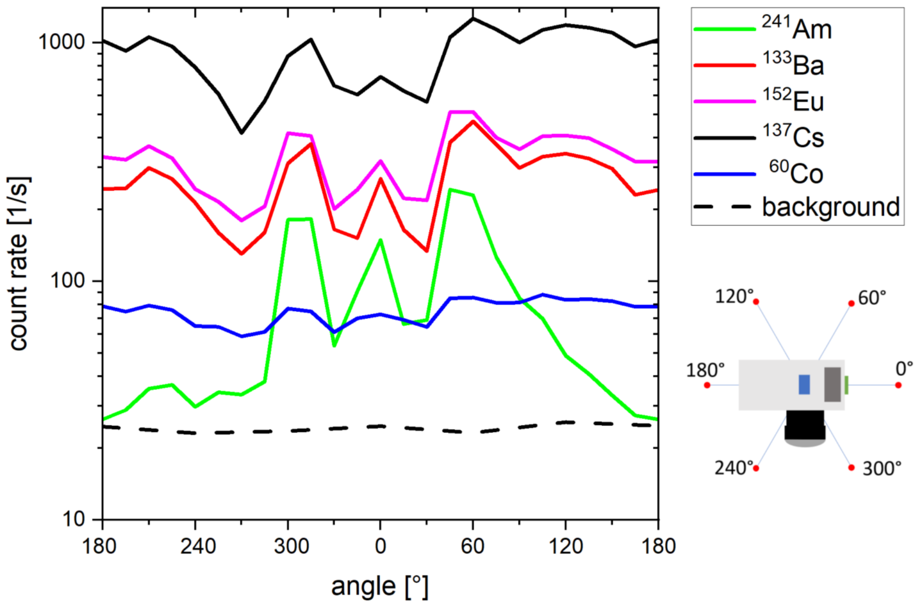

Figure 11: Count rates measured during scans for the different nuclides and background scan. Angles concerning the orientation of the detector and the source are the same as in Figure 1 and are given on the right.

6 CONCLUSIONS AND FURTHER RECOMMENDATIONS

The measurement result is strongly dependent on the source strength. At lower dose rates, it is necessary to determine the count rate to assess whether a source is present. If a count rate above background level is observed, it confirms the presence of a radiation source although this source is not necessarily located or identified.

For higher dose rates a good starting point for an unknown setting is one long-term measurement using Compton scattering imaging with a 360° FOV, to identify the location of the radiation source. For single sources specific patterns emerge based on the source's position relative to the detector.

During scanning, if the detection limit is adequate, the radiation source can be located and identified. The measured dose rate depends on the absorption inside the detector due to the mask, electronics and holder material. Regardless of the type of gamma camera used, it is essential to consider the internal geometry and account for internal shielding to ensure that the results are interpreted correctly.

In coded mask imaging, the field of view is 45°. After a rough localization using the Compton imaging this method with the higher spatial resolution can be used to obtain a more accurate measurement in this previously determined approximate direction. Therefore, it is highly beneficial to use a combined gamma camera that features both a 360° FOV component with potentially lower resolution and a higher resolution component with a narrower FOV.

The spatial resolution seems to be dependent on the kind of sources, two sources of different nuclides seem to be easier to localize than two sources of the same nuclide. This might be due to the reconstruction calculation and would be therefore valid for all such gamma cameras. This will be examined in more detail in the future as well as scans shall be done without a constant distance towards the source like in the present work, but with comparable dose rates in order to examine the effect of correct identification in more detail. As only sources with relative low dose rates are available the measurement duration will have to be enlarged.

7 REFERENCES

[1] Ghelman, M., Kopeika, N., Rotman, S., Edvabsky, T., Vax, E. and Osovizky, A. „Design of 4π Directional Radiation Detector based on Compton Scattering Effect“, EPJ Web Conf. Volume 253. ANIMMA, 2021. Available at: https://doi.org/10.1051/epjconf/ 202125307003.

[2] Parajuli, R.K., Sakai, M., Parajuli, R. and Tashiro M. „Development and Applications of Compton Camera—A Review“, MDPI 2022. Available at: https://doi.org/10.3390/s22197374 .

[3] NuviaTEC-Instruments, NuVISION Datasheet. Available at: NVG-375045-FicheNuVISION-DE-Nov2020-1.pdf (nuviatech-instruments.com).

Note: All digitally available sources were last accessed on June 21, 2024.